Stanford Exploration Project, Report 65, January 13, 1998, pages 1–17

Velocity estimation using prestack depth migration: field data trial

John T. Etgen[1]

keywords: *modeling, velocity, prestack*

ABSTRACT

Velocity information extracted from prestack migrated data can be used to update the interval velocity model by solving a filtered tomography problem. Depth migration with the new velocity model should yield an improved structural image that stacks better over offset. Initial field data results indicate the promise of the method and also point out some of the difficulties encountered when using it.

INTRODUCTION

In previous reports (Etgen, 1989, 1988), I detailed a method for estimating interval velocities using prestack depth migration and residual prestack migration. Amoco and Seismograph Service Limited (SSL) have provided me with a dataset to test this velocity estimation method. The dataset is from the North Sea and has a salt dome and other structure that causes lateral velocity variation. I wanted a dataset that had significant lateral velocity variation, but one where the lateral variation wasn't so severe that it was difficult to get any image at all or that I had to know anything about local geology or needed well logs to solve the problem. Furthermore, I wanted a dataset that wasn't dominated by deconvolution or noise problems. The dataset I received appears to meet these requirements.

This paper describes the data and my initial attempt at deriving an interval velocity model that gives a good prestack depth migration of the data. After migration with a velocity model $v(z)$, the data had residual moveout indicating errors in the velocity model. Tomographic back-projection of those errors using the method I presented in previous reports gives an update to the velocity model in the form of a change in interval slowness.

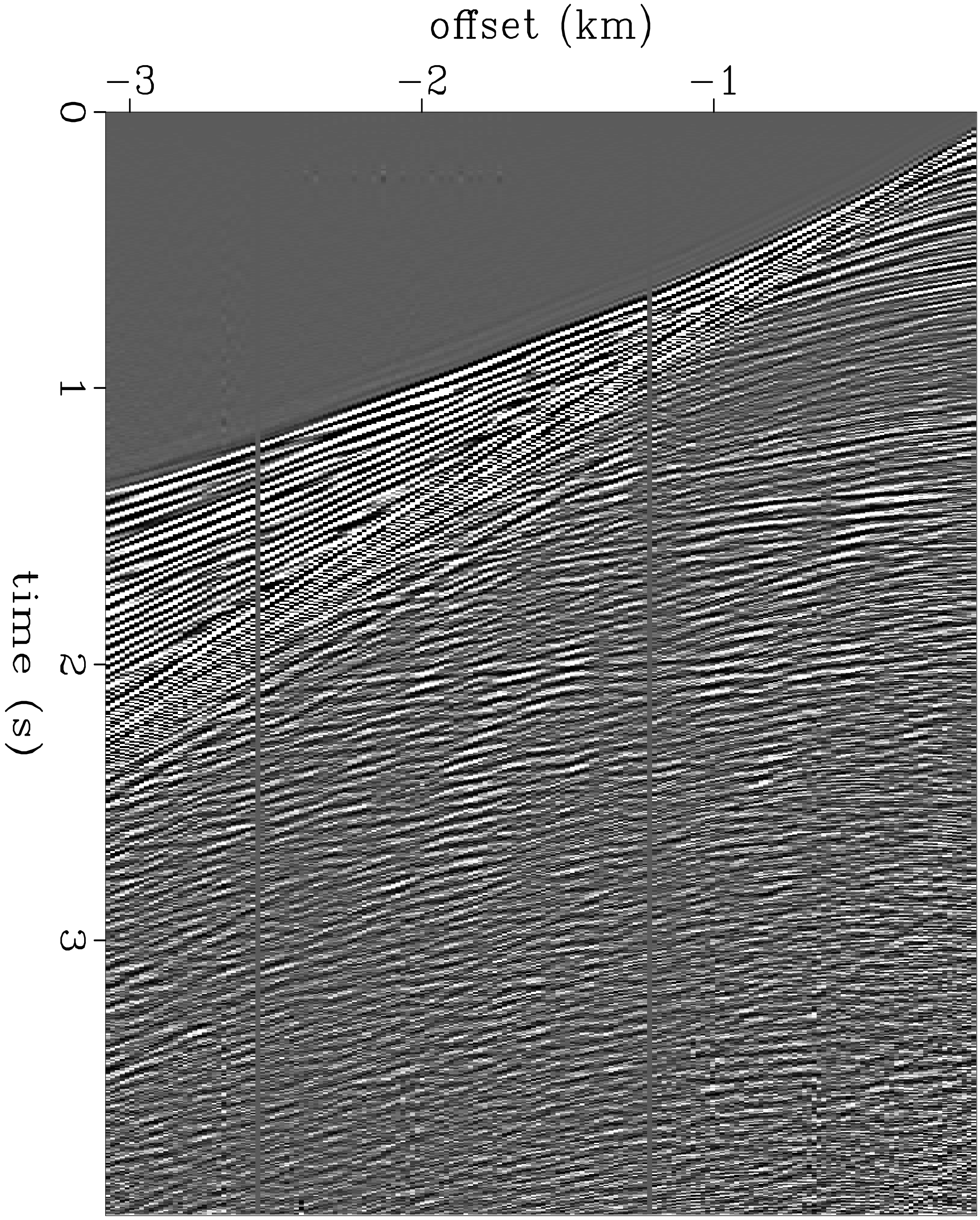

Figure 1: A shot profile from the dataset. Note the refracted waves at large offsets. The data have been gained by $t^{1.5}$. $\boxed{\text{john-one.shot}}$ [NR]

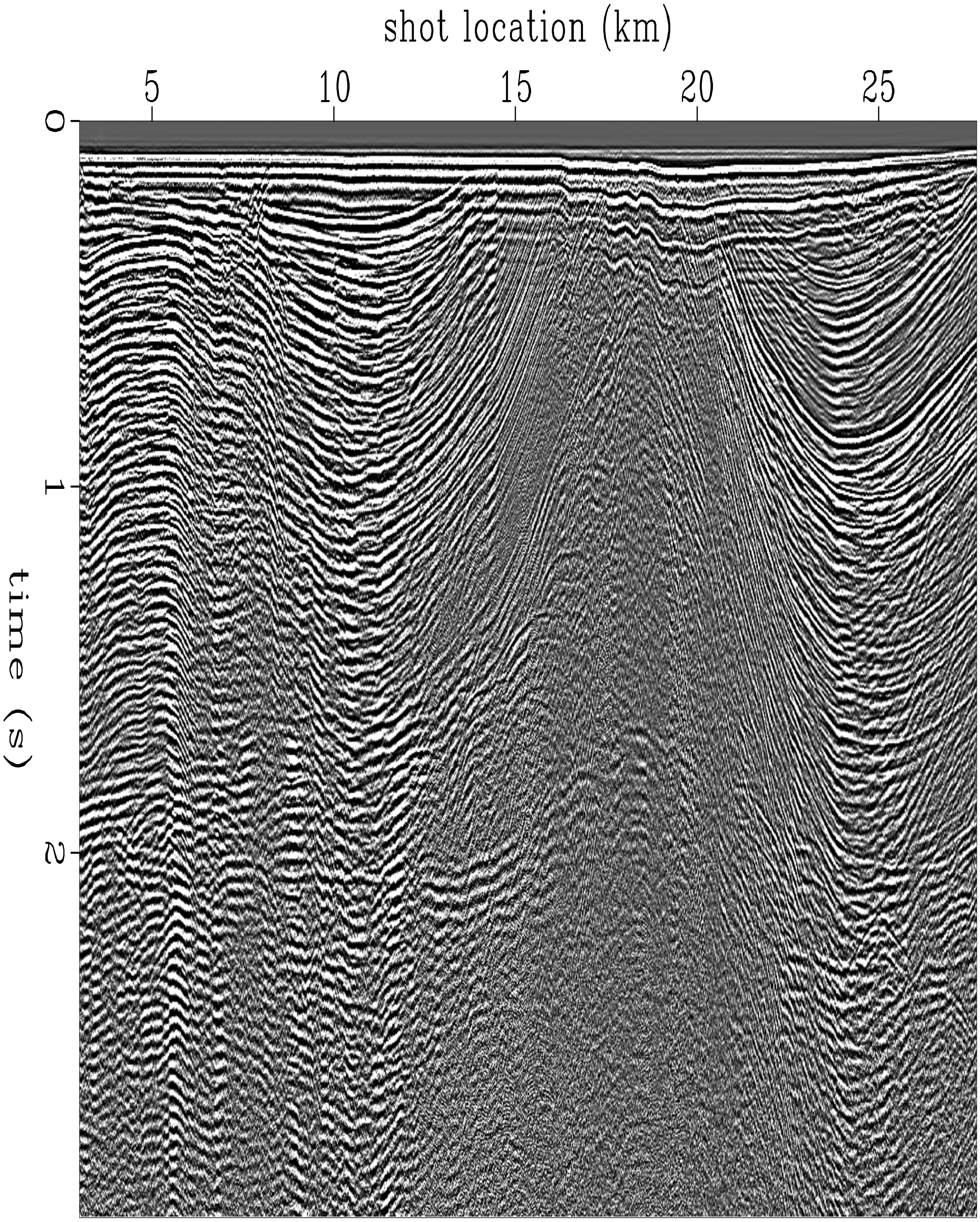

Figure 2: The near-offset section of the data. Note water-bottom multiples and pegleg multiples after some of the deeper reflectors. john-co.inner.pre [NR]

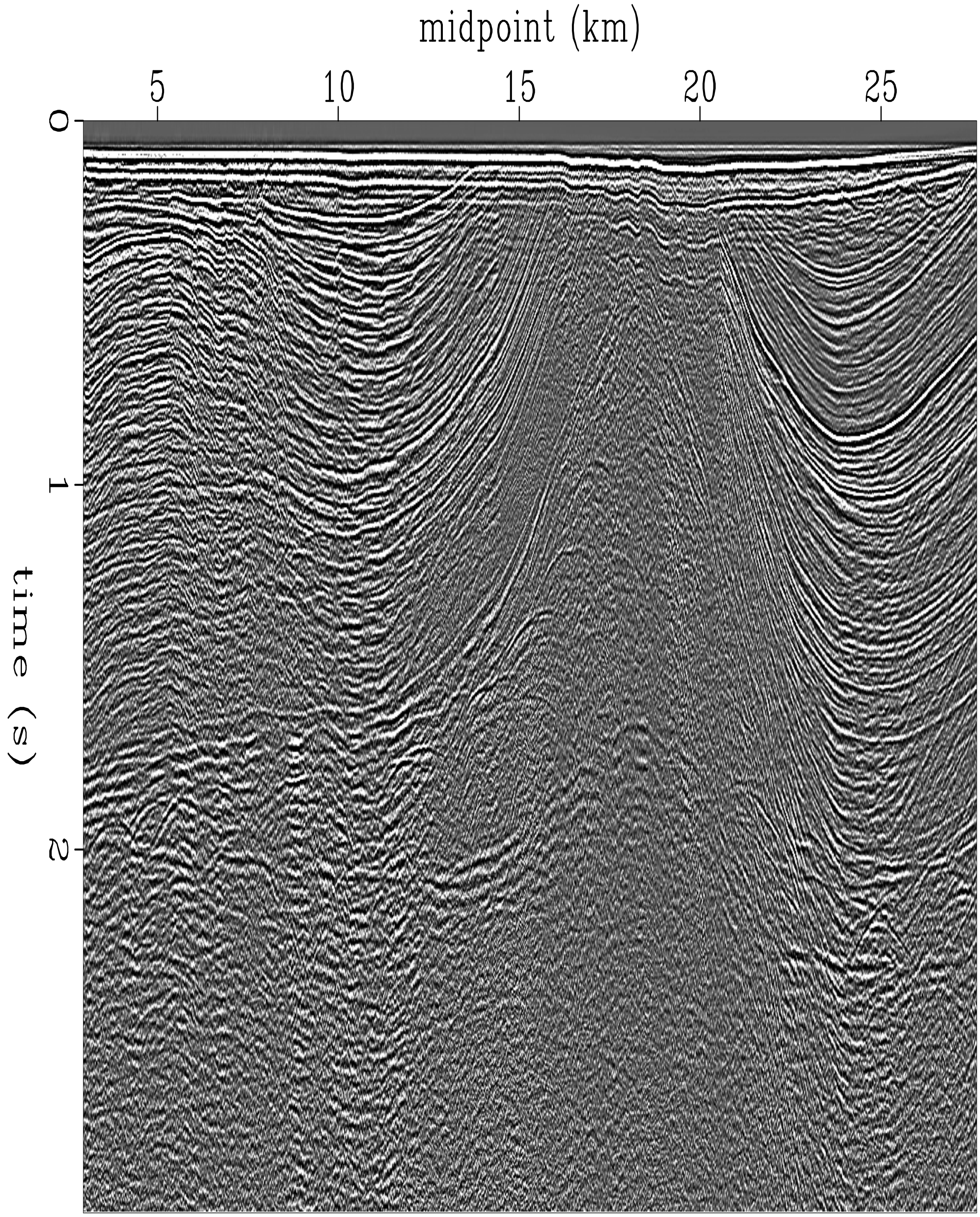

Figure 3: The same near-offset section as in Figure 2, now after gapped decon. Some of the water-bottom multiples have been attenuated and the pegleg multiples are attenuated. john-inner.co.section.decon.raw [NR]

THE DATASET AND ITS PREPROCESSING

Figure 1 shows a shot profile from the dataset. The profile was plotted with $t^{1.5}$ gain. The first processing step after reading the tapes and examining the shot profiles was to retain only the inner 120 out of 180 total offsets. The outermost offsets had poor signal to noise and all but the deepest reflectors were swamped by refracted energy. Next, I sorted the data to constant-offset sections and muted the refractions and other steep angle arrivals. Figure 2 shows the near-offset section of the data. Water bottom and pegleg multiples are evident in Figure 2, so I ran single-trace gapped decon on the data. Figure 3 shows the same section as in Figure 2 after gapped decon. Unfortunately, the gapped decon did not remove the water-bottom multiples especially on the nearest offsets. This may adversely impact my ability to use velocity information in the shallow part of the section. I speculate that near offset reflection and multiples were near, at, or beyond critical angle (depending on how many bounces). The water bottom is shallow (60-70 m) and apparently hard since the velocity increases rapidly. This results in amplitude relations between the different order multiples that are not predictable using a 1-D model for wave propagation.

The gapped decon did do an excellent job removing a lot of the "ringy" appearance of the near-offset sections particularly for midpoints from 1–12 km. Gapped decon did removed or attenuate the pegleg multiples of the deeper reflectors. Compare the bottom-of-salt reflector on Figures 2 and 3.

After decon the data were bandpassed to an upper frequency of 80 Hz. This relaxed spatial aliasing constraints on the migrated output so a coarser output sampling could be used.

Initial prestack depth migration

I constructed a crude interval velocity model that varied with depth only from the stacking velocities on the paper plot that came with the data tapes. Figure 4 shows the velocity model. I migrated all constant-offset sections with this velocity. The migrated constant-offset sections were binned into groups of three and stacked, reducing the data volume and improving signal/noise. The resulting sections were saved to be used for velocity analysis. Figure 5 shows the stack of the nearest three migrated constant-offset sections. The pull-up effect of the high-velocity dome on the bottom of salt reflector is still evident because the interval velocity model used for migration didn't "know" about the salt.

Figure 6 shows four selected post migration common-midpoint gathers. Varying amounts of residual moveout are evident. The signal quality of the base-of-salt reflection is poor for the midpoint beneath the thickest part of the dome, but hopefully there will be enough velocity information to get a meaningful update from the inversion algorithm. Figure 7 shows the stack of migrated constant-offset sections.

[1]**email:** not available

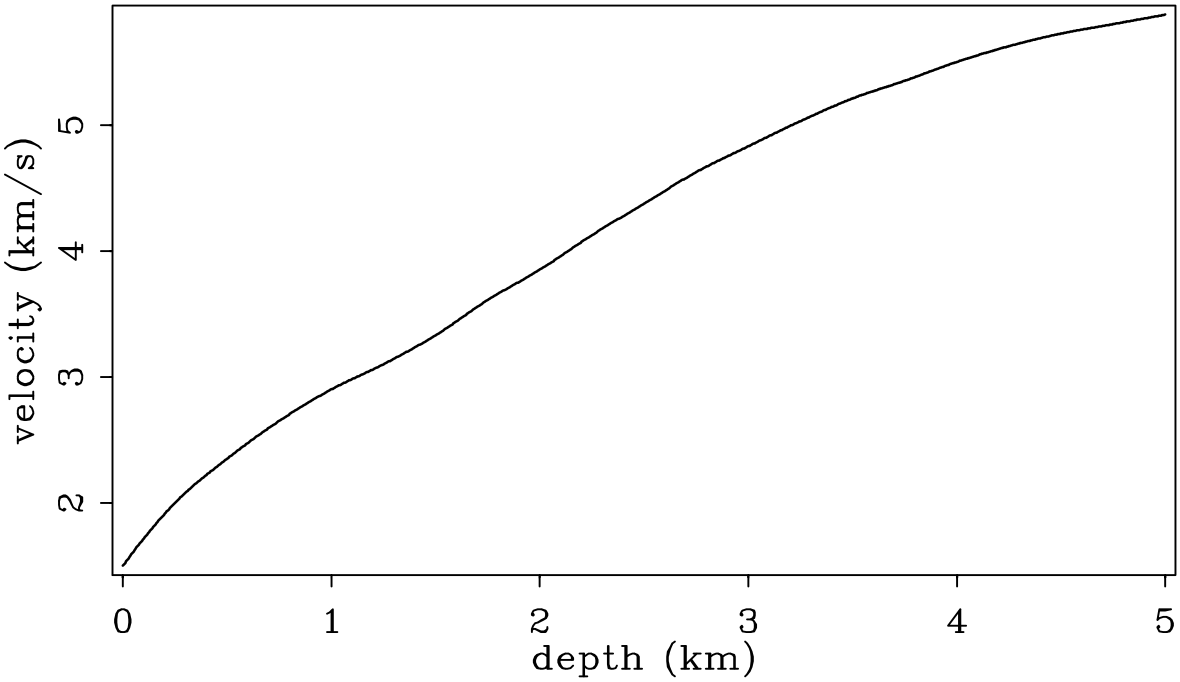

Figure 4: The velocity model, a function of depth only, used for the initial prestack migration of the dataset. john-vozkm.raw [NR]

Despite the velocity errors evident in Figure 6, prominent events can still be identified. This illustrates one of the advantages of using an intermediate quantity like residual NMO+DMO stacking velocity (Etgen, 1989) over directly picking event locations. It would be difficult to pick robustly the images of reflectors on individual sections; stacking can improve the reliability of the velocity information in the data. This will be even more evident on the residual NMO+DMO semblance panels in Figure 8.

ESTIMATING A NEW SLOWNESS MODEL

Now that the data have been migrated, and velocity errors are evident, use the following algorithm to compute an update to the interval slowness model.

Outer loop over interval slowness models $\mathbf{w}_i$

{

Migrate the data with $\mathbf{w}_i$

Apply residual NMO+DMO: compute $S(\gamma, \tau)$

Estimate dips on the stacked image

Pick important reflector points

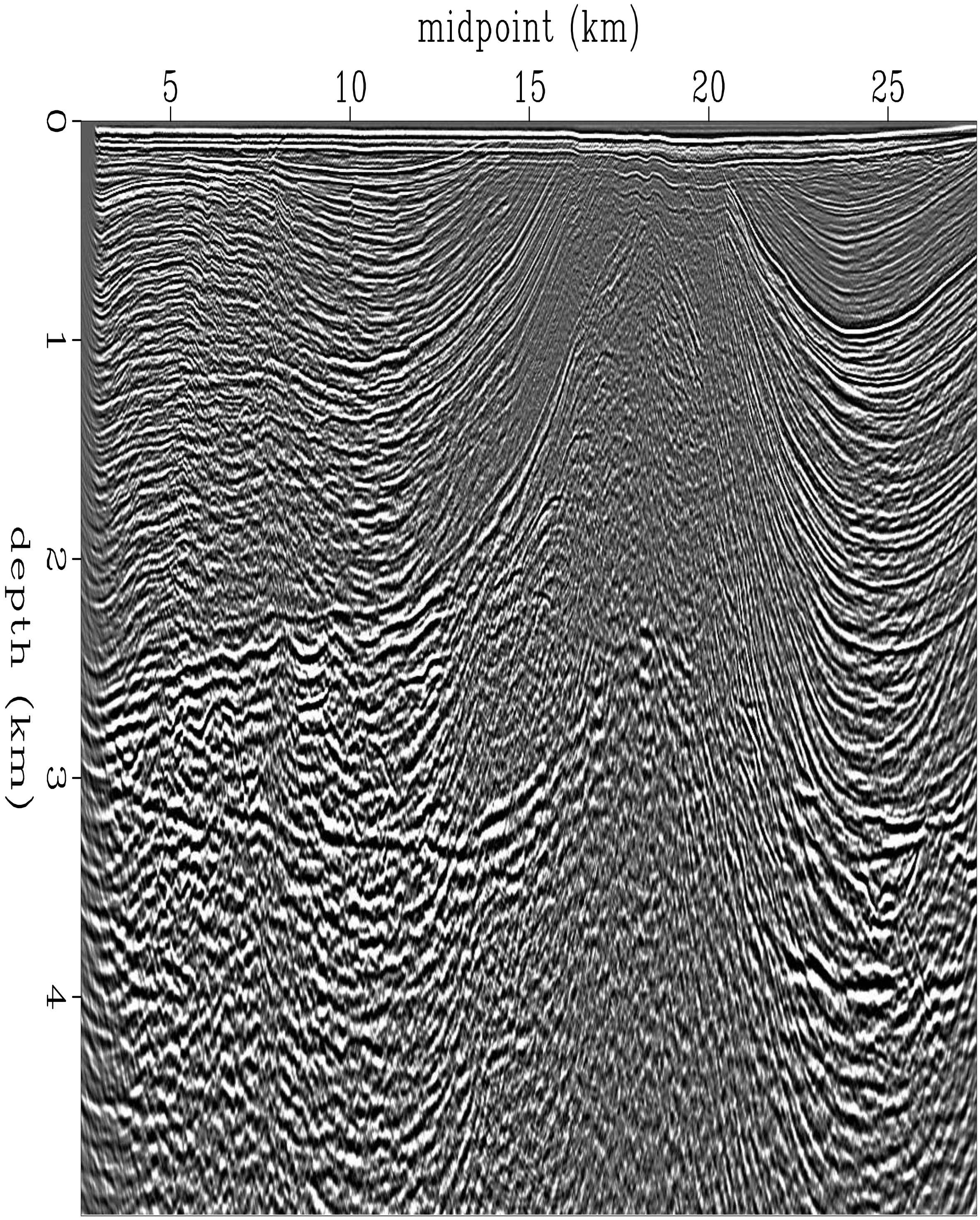

Figure 5: Migrated and stacked section obtained from the 3 nearest offsets. Partial stacking was used to reduce the data volume and because the individual constant-offset sections are spatially aliased. john-mig.co.inner.raw [NR]

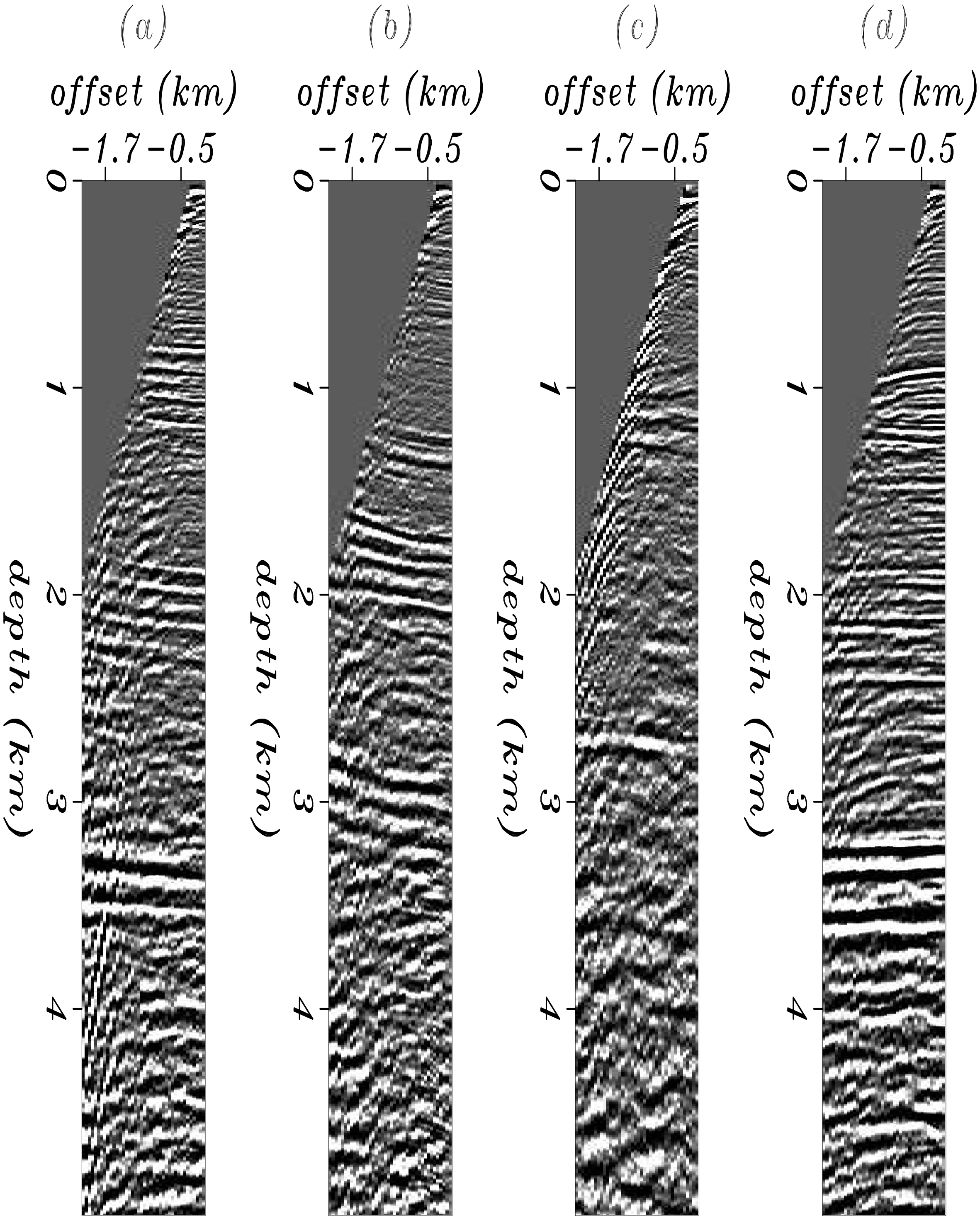

Figure 6: Four post-migration common-midpoint gathers. Each displays a different amount of residual moveout and different signal/noise ratio. (a) is the midpoint at 13.3 km; (b) is the midpoint at 15.6 km; (c) is the midpoint at 19.8 km; (d) is the midpoint at 25.3 km. john-mig.cmps.combined [NR]

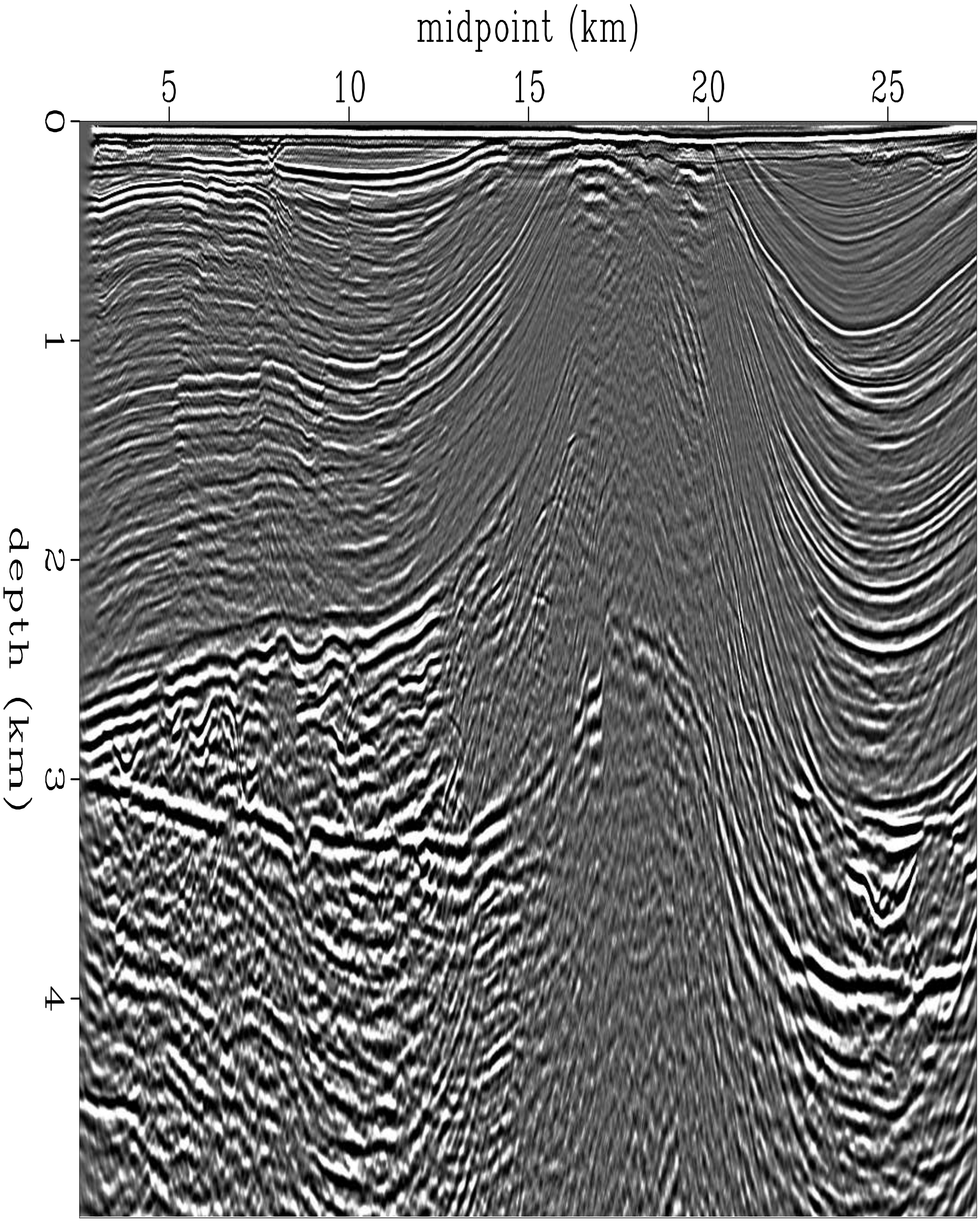

Figure 7: Stacked section of all migrated constant-offset sections. Even though residual moveout is large for some midpoints, prominent reflectors can still be identified. john-mig+stack.raw [NR]

Compute the operator $\mathbf{G}$

$\Delta\mathbf{w}_0 = \hat{\alpha}\nabla_{\mathbf{w}}Q$; j=1

While $\|\Delta\mathbf{w}\| < 20\%$ and $\nabla_{\mathbf{w}}Q > 0$

{

Compute $\nabla_\gamma Q$

$\nabla_{\mathbf{w}}Q = \left[G_\gamma^T - \frac{\delta\gamma}{\delta\tau}G_\tau^T\right]\nabla_\gamma Q$

line search $\Delta\mathbf{w}_j + \alpha\nabla_{\mathbf{w}}Q$

line search $\Delta\mathbf{w}_{j-1} + \beta(\Delta\mathbf{w}_j - \Delta\mathbf{w}_{j-1} + \hat{\alpha}\nabla_{\mathbf{w}}Q)$

Update $\Delta\mathbf{w}_{j+1} = \Delta\mathbf{w}_{j-1} + \hat{\beta}(\Delta\mathbf{w}_j - \Delta\mathbf{w}_{j-1} + \hat{\alpha}\nabla_{\mathbf{w}}Q)$

Update reflector position map $x(\tau)$,$z(\tau)$, $\delta\gamma/\delta\tau$

$j = j + 1$

}

$\mathbf{w}_{i+1} = \mathbf{w}_i + \Delta\mathbf{w}_{\text{final}}$; $i = i + 1$

}

The objective function Q is the sum of the semblance $S(\gamma(\mathbf{w}), \tau)$ over events. $\mathbf{G}$ is the relation between changes in the interval slowness model $\mathbf{w}$ and changes in γ the residual slowness of the chosen reflection events. $\nabla_\gamma Q$ finds the direction and magnitude of increasing semblance versus γ for each reflector. $\delta\gamma/\delta\tau$ guides the change in γ due to reflector movement. The line searches return the values $\hat{\alpha}$ and $\hat{\beta}$ to describe the maxima of the objective function in their respective search directions. The conjugate-gradient algorithm I use is called PARTAN and is described by Luenberger (1984). The algorithm is robust for nonlinear functions and when line searches are inexact. This is important because my objective function is non-quadratic in shape and for values of γ intermediate to those computed the objective function has to be computed by interpolation. The bound on the magnitude of the change in interval slowness is taken with respect to the interval slowness model used for migration. 20% is not meant to be taken as a firm figure; the data should be remigrated once residual migration can no longer adequately describe the reflector movement that accumulates as the iterations proceed. Also, the norm measuring relative change in the slowness model can be an $\mathbf{L}_\infty$ or $\mathbf{L}_2$ norm.

Residual slowness analysis

After migration, the first step to estimating a new interval slowness model is to apply residual NMO+DMO to the constant-offset sections. If the data do not stack best for $\gamma = 1$ then moveout is still present over offset which implies velocity errors. I

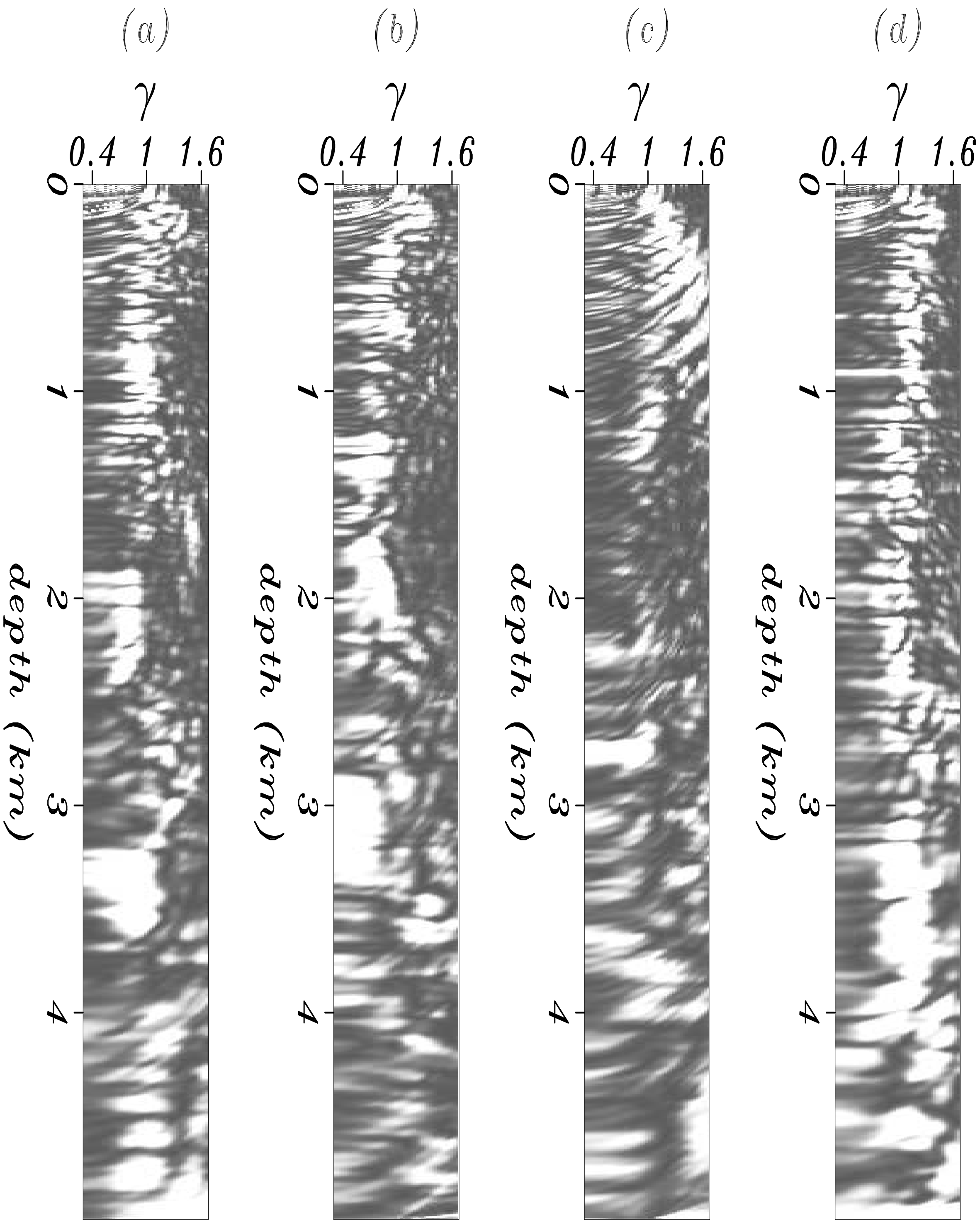

Figure 8: Residual NMO+DMO semblance panels for the four midpoints of Figure 6.
john-combined.semb [NR]

calculated the stack semblance for a range of γ; $.3 < \gamma < 1.68$ by applying residual NMO+DMO to the migrated constant-offset sections. Figure 8 shows semblance versus residual slowness γ, for the same four midpoints of Figure 6.

Selecting prominent reflectors

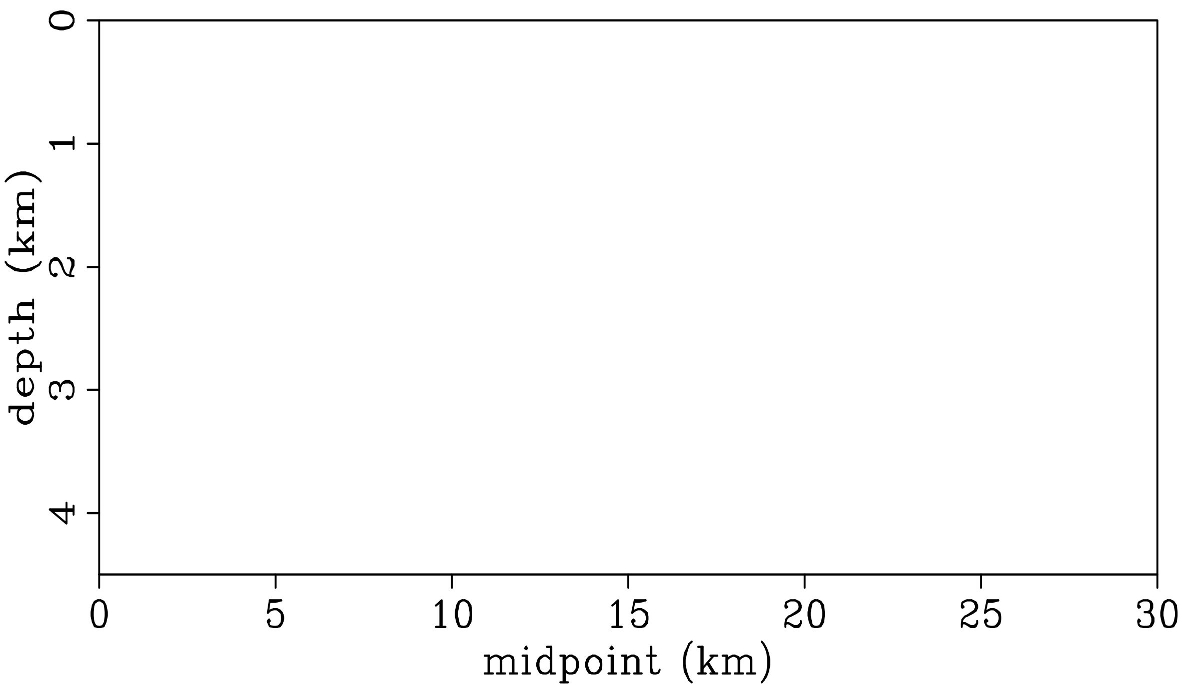

Figure 9: The reflector points used in the velocity estimation algorithm. The objective function is obtained by summing the semblance at the appropriate value of γ for each of these reflector points. john-pixe.xzkm [NR]

The dips of events in the stacked section are needed for the computation of **G** and can be obtained by computing local dip spectra and picking the maxima. The velocity information of nearby reflector points with the same dip is redundant especially when the velocity varies smoothly laterally. Selecting a sparse set of reflector points to use in the computation of the objective function reduces the cost of the inversion. The reflector points that were chosen were locally maxima in dip semblance and had high minimum entropy norms (Berkhout, 1984) of their dip spectra. It is especially worthwhile to try to select points sparsely normal to the dominant dip and enhance continuity along the dip direction. The picking algorithm penalizes nearby picks in the direction normal to the dominant dip and encourages picks that form continuous prominent reflectors. For the first run of the inversion I also chose not to pick shallow events. Figure 9 shows the reflector points that were picked and used for updating the interval slowness model.

Running the inversion algorithm

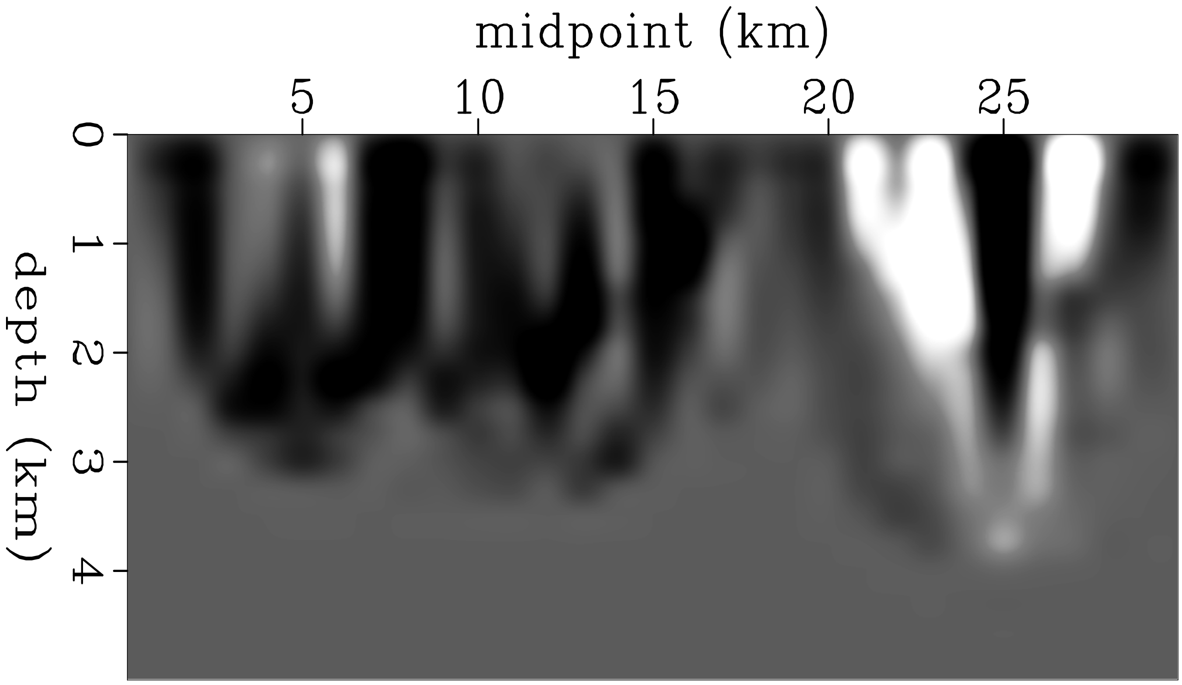

Figure 10: The initial gradient of the stack semblance for the picked events tomographically back-projected into the model space by $\mathbf{G}^T$. john-datag.first [NR]

Figure 10 shows the initial gradient of the objective function with respect to the interval slowness model (taken with $\gamma = 1$). This plot is the first iteration of a tomographic back-projection of the velocity errors. This gradient gives an idea of what parts of the model have errors and how changes in those parts of the model affect the stack semblance of the data.

The PARTAN algorithm was run for 30 iterations and stopped when the gradient of the objective function with respect to γ was approximately zero. Figure 11 shows the cumulative change in the interval slowness model obtained.

Post mortem

The update to the interval slowness contains rapid lateral variations. These variations have a wavelength approximately the same as the cable length (2 km). The slowness model had a node spacing of 1 km horizontally and .25 km vertically. While some of these variations may be actual features of the true interval slowness model, it is more likely that they are artifacts. Gaps in reflector point coverage and variations in quality of velocity information are possible causes (Fowler, 1988). The shape of the multiples in Figure 2 do indicate some short wavelength features (less than a cable length), and eventually these features can be estimated; but for an initial update after a migration with $v(z)$, it is best to try for a laterally smooth update.

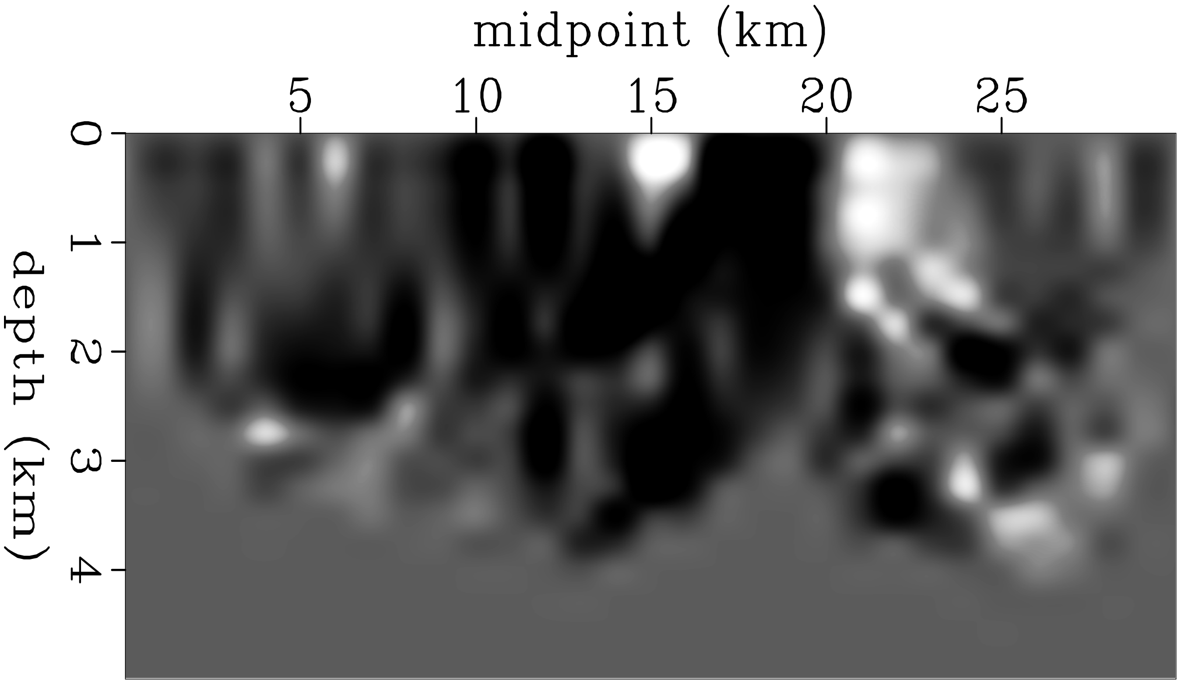

Figure 11: Estimated change to the interval slowness model after 30 iterations of the velocity estimation algorithm. The inversion stopped when $\nabla_\gamma Q \approx 0$, that is, when all residual moveout had been explained. john-deltaw.lastiter [NR]

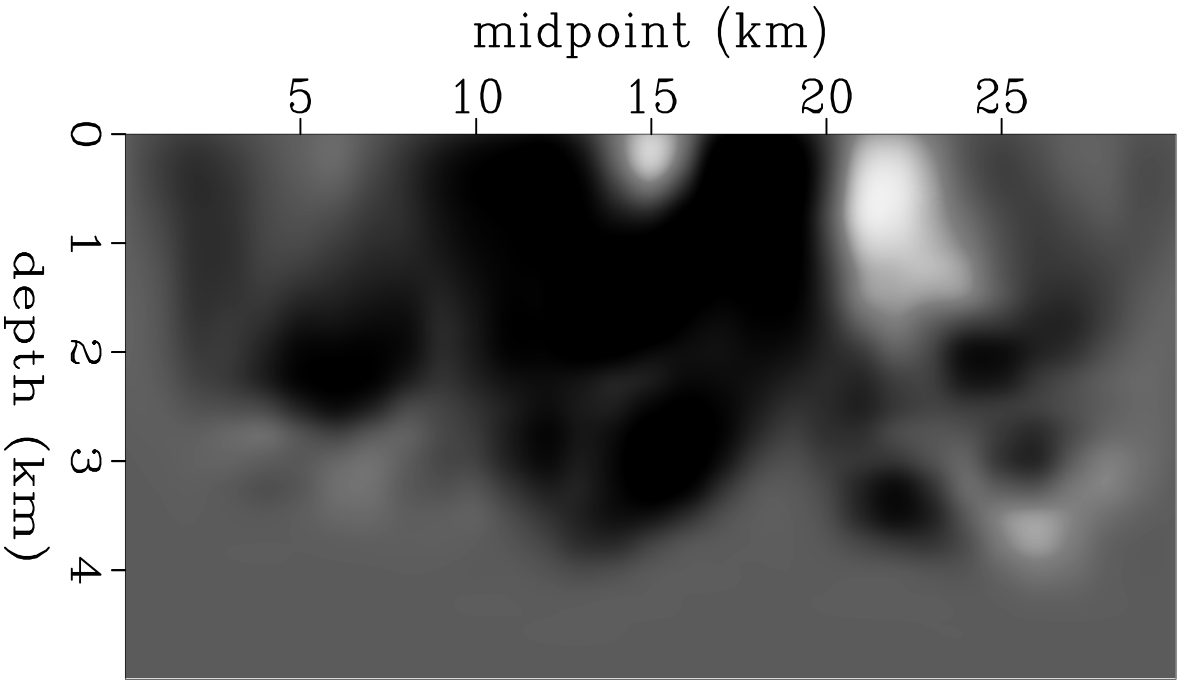

Figure 12: A smoothed version of the update to the model in the previous figure. The smoothing was over 3 nodes laterally and vertically. This removes the features that resonate with the cable leaving only features with lateral wavelengths longer than the cable. john-deltaw.smoothed [NR]

For the example shown, the inversion was unconstrained and no model covariance matrix was used. Smoothing the result show in Figure 11 gives the slowness model update shown in Figure 12. The low wavenumber change to the background model is more evident. It would have been more correct get a smoother update by including a model covariance matrix in the inversion. I will do this in the future.

It is encouraging that the algorithm recognized the slowness decrease (velocity increase) we would expect over and around the dome where deeper, faster rocks are thrust up. The next step is to remigrate the data from scratch with the new velocity model and see if the stack is better and if the structural image improves.

CONCLUSIONS

Residual NMO+DMO applied after an initial prestack migration indicates that there is information about the lateral variation of the velocity of the subsurface contained in the dataset shown. Inversion of the relation between residual slowness and interval slowness gives an update to the interval slowness model used for the initial prestack migration. The higher lateral wavenumbers of this update are probably unreliable, due to non-uniform reflector coverage and near-sea-floor effects. The lower lateral wavenumbers give a physically plausible and intuitive change to the slowness model. I make the usual disclaimer, more investigation is needed.

ACKNOWLEDGMENTS

I thank Amoco and SSL for releasing the dataset to SEP.

REFERENCES

De Vries, D., and Berkhout, A. J., 1984, Velocity analysis based on minimum entropy: Geophysics, **49**, 2132–2142.

Etgen, J., 1989, Kinematic residual prestack migration: SEP–**61**, 79–102.

Etgen, J., 1989, Velocity analysis using prestack depth migration: applying the linear theory: SEP–**60**, 25–40.

Etgen, J., 1988, Prestack depth migration velocity analysis: linear theory revised: SEP–**59**, 121–140.

Fowler, P., 1988, Seismic velocity estimation using prestack migration: PhD Thesis, Stanford University; also SEP–**58**, 1–185.

Luenberger, D.G., 1984, Linear and nonlinear programming (2nd edition): Addison-Wesley Publishing Company Inc., 254–257.